

# I Session: JUPITER, AS OBSERVED AT LONG RADIO WAVES

## The Decametric Radio Emissions of Jupiter

G. R. A. Ellis

Physics Department, University of Tasmania, Hobart, Tasmania

The present state of knowledge of the decametric radio emissions of Jupiter is reviewed. Theories of the radiation are discussed and their implications concerning the general environment of Jupiter and the properties of the Jupiter magnetosphere are examined. The survey reveals the need for more observations and additional work on the theory.

### 1. Introduction

The discovery of the decametric radio emissions of Jupiter in 1954 by Burke and Franklin [1955] and the subsequent observation of the microwave radiations of the planets has provided, in principle, a means of acquiring new and otherwise unobtainable information about the planetary surfaces, atmospheres, magnetic fields, and environments. However, the full utilization of these natural information channels requires not only the accumulation of sufficient observational data but also the development of satisfactory theories of the origin of the radiation. That is, it must be possible to decode the signals. In the case of Jupiter, such developments have reached an advanced stage. Since 1954 a great quantity and variety of data have been obtained. A number of theories of the origin of the radiation have been advanced and the application of the theories, together with the data, is leading to the study of the planetary environment.

This paper surveys recent progress and the present state of knowledge of Jupiter as deduced from the decametric emissions.

### 2. The Observations

#### 2.1. Fine Structure and Power Spectrum

The radiation is observed to occur in short bursts with a duration of the order of a second, and in the frequency range from less than 5 Mc/s to 43 Mc/s [Shain, 1956; Kraus, 1958; Ellis, 1962]. The bursts are most easily observed near 20 Mc/s. At higher frequency their intensity and rate of occurrence decrease rapidly, while at lower frequencies the opacity of the terrestrial ionosphere makes observations difficult.

The radiation is sporadic and the bursts are generally grouped together in storms lasting from a few minutes to several hours. The durations of the bursts them-

selves range from 0.001 sec to several minutes [Riihimaa, 1964a; Douglas and Smith, 1961; Shain, 1956]. Dynamic spectrograph observations of the variation of the intensity of the radiation with frequency and time shows that at any instant the bandwidth of the bursts may be as small as  $\frac{1}{2}$  Mc/s, while the center frequency of the group of bursts may change slowly (approximately 1 Mc/s per min) with frequency either in the positive or negative sense. Examples of spectra with a time resolution of 1.3 sec are shown in figure 1d [Warwick, 1963a]. With higher time resolution, the individual burst structure in the spectrograms becomes visible and much higher rates of frequency change can be observed (figs. 1a, b, c) [Riihimaa, 1964a, 1964b].

The intensity of the bursts often exceeds that of any other discrete cosmic radio source with the exception of the disturbed sun. Within the observed frequency range, the spectrum shows a rapid and monotonic decrease in intensity with increasing frequency. Figure 2 shows the spectrum of the average flux density [Ellis, 1962; McCulloch and Ellis, 1965]. The total power emitted by the planet is estimated to be  $5 \times 10^{10}$  W [Carr et al., 1964].

#### 2.2. Periodicities

##### a. Longitude Profiles

The number of bursts and their mean power are observed to vary with rotation of Jupiter [Shain, 1956; Carr et al., 1961; Gallet, 1957; Douglas, 1960]. The rotational profile of burst number shows a number of peaks, and the whole pattern is recurrent with a period of approximately 9 hr 55 min 29.37 sec. Determinations of the period using data over 9 years were made by Douglas [1960] and Carr et al., [1961]. From an exhaustive statistical analysis, Douglas determined the value 9 hr 55 min 29.37 sec  $\pm$  0.13 sec for the length of the sidereal day, while Carr et al., found 9 hr 55 min 29.35 sec. Douglas [1960] and Gallet [1961] have

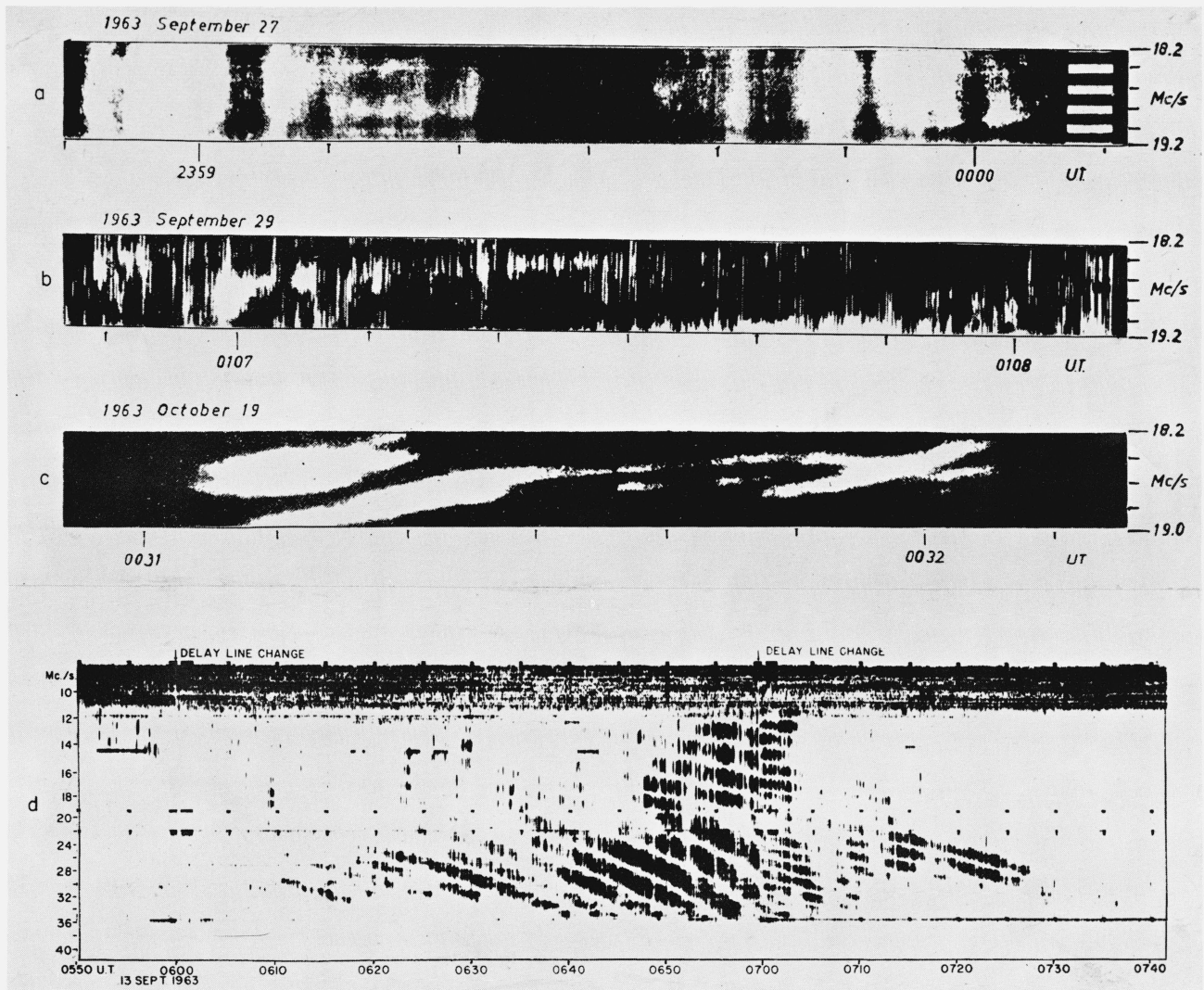


FIGURE 1a. Spectrograms, recorded by Riihimaa [1964] with a time resolution of 0.1 sec.

FIGURE 1b. Spectrograms, recorded by Riihimaa [1964] with a time resolution of 0.1 sec.

FIGURE 1c. Spectrograms, recorded by Riihimaa [1964] with a time resolution of 0.1 sec.

FIGURE 1d. Frequency-time spectrogram recorded with an interferometer fringe pattern [Warwick, 1963a].  
Time resolution 1.3 sec.

considered the consistency of this period—Gallet suggested that there was evidence that the period 1956–1957 was approximately 1 sec longer than the mean period from 1951–1957, but Douglas found no statistically significant variations.

For presenting longitude profiles of the emission it is clearly desirable to use a system of longitudes rotating with the period. In this review we use the System III (1957) longitudes recommended by the International Astronomical Union in 1962. The sys-

tem rotates with the period 9 hr 55 min 29.37 sec, and coincides with System II longitudes at 0 hr UT on January 1, 1957. An ephemeris of the central meridian longitude on this system for the years 1961–1963 has been given by Morrison [1962].

Longitude profiles showing the probability of emission as a function of the longitude of the central meridian of the planet have been given by many investigators, beginning with Shain [1956]. The profiles vary with frequency. Near 20 Mc/s a prom-

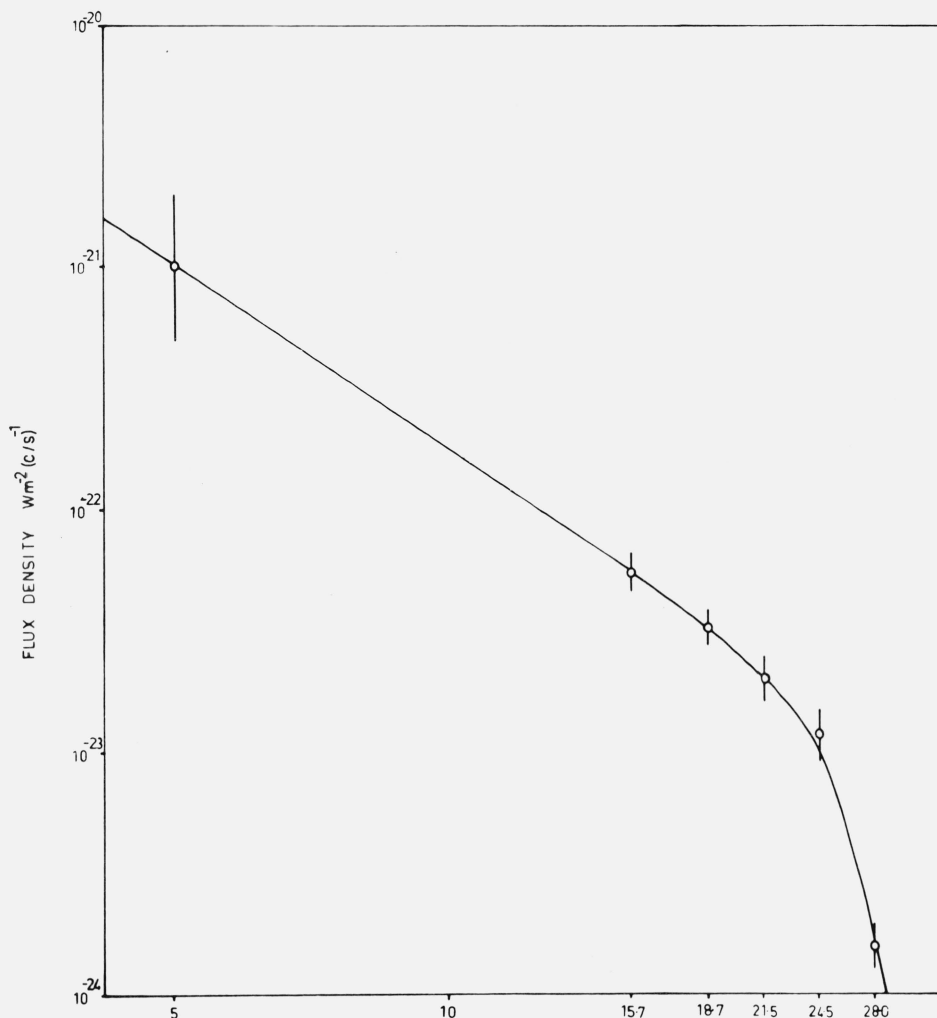


FIGURE 2. Mean flux density spectrum [McCulloch and Ellis, 1965].

inent peak is observed between  $\lambda_{\text{III}} = 200^\circ$  and  $280^\circ$ , and a secondary peak between  $90^\circ$  and  $160^\circ$ . At higher frequencies, the longitude width of the peaks decreases while at lower frequencies the probability of occurrence ceases to be a strong function of longitude. At 5 Mc/s, bursts are observed almost independently of the aspect of the planet. The profiles of mean power resemble those of the rate of occurrence, except that the variations with longitude are more pronounced. At 5 Mc/s, for example, the mean power profile shows a quasi-sinusoidal variation with peaks near  $160^\circ$  and  $330^\circ$ . Figure 3 shows probability and mean power profiles for different frequencies.

Direct observation of the simultaneous variation of the intensity with frequency and time by Warwick [1963b] has shown that the frequency-time spectrograms also repeat with planetary rotation. Warwick noticed a tendency for the center frequency of the

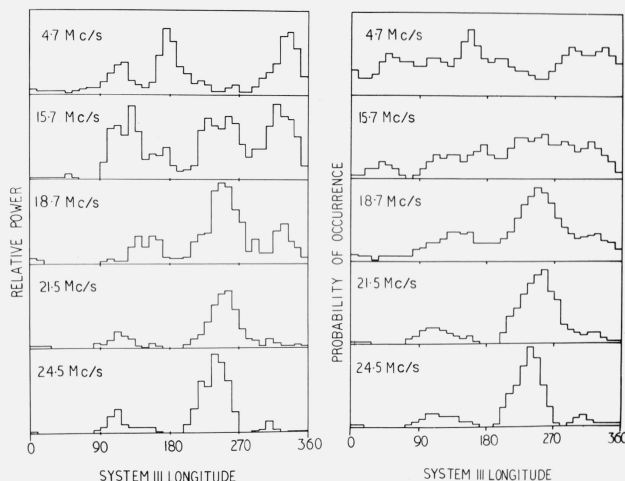


FIGURE 3. Longitude profiles of occurrence and mean power of bursts [McCulloch and Ellis, 1965].

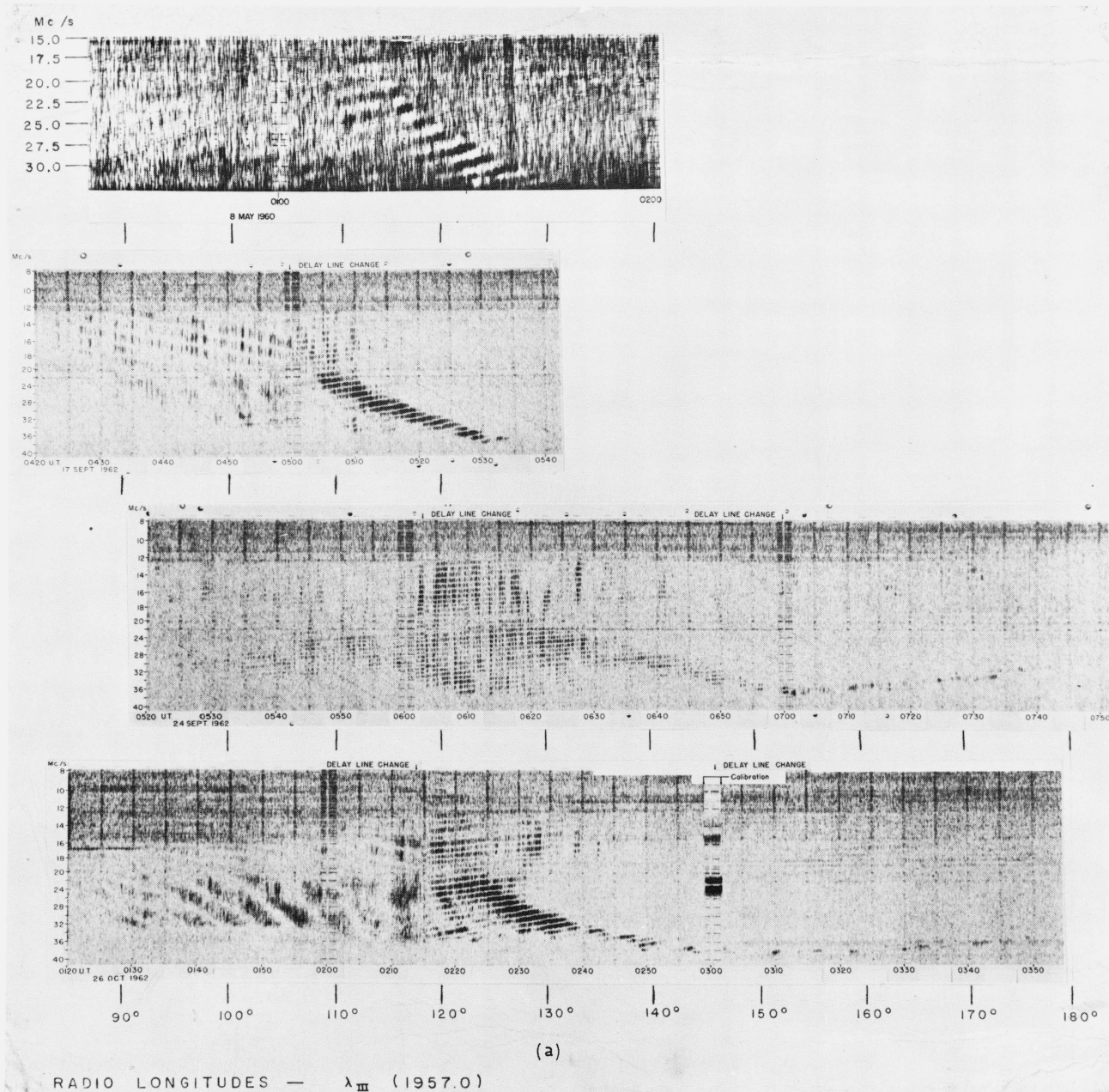


FIGURE 4. Spectrograms showing long-term repeatability of frequency-time variation near longitude 120° System III. Frequency 8–40 Mc/s downwards in lower three sections [Warwick, 1963b].

emissions to increase with time in the longitude region near 130° and to decrease with time near 270°. The features which recur have durations of several minutes to an hour. Figure 4 shows the striking repeatability of the  $f$ - $t$  patterns near longitude 130° over a period of 2 years.

A composite frequency-longitude diagram using the data of Warwick and the single-frequency data of figure 3 is given in figure 5. A notable feature is the disappearance of the intensity peaks near 130° and

240° as the frequency decreases below 10 Mc/s. At the same time, the peaks near 175° and 330° become more pronounced.

#### b. Satellite Periodicities

As well as varying with the rotation of Jupiter, the rate of occurrence of bursts is observed to contain longer periods. These have been investigated by Bigg [1964], who showed that, in particular, a prom-



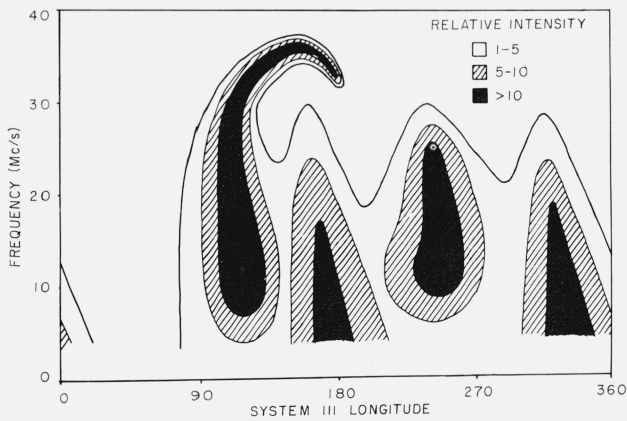


FIGURE 5. Composite frequency-longitude variation of integrated burst power.

inent periodicity is associated with the orbital position of the satellite Io. This is illustrated in figure 6. The 130° and 230° peaks in the System III profiles near 20 Mc/s are clearly seen to be observable almost exclusively when Io is about 90° and 240° from superior

conjunction respectively. The data of Ellis [1962] at 4.7 Mc/s and McCulloch and Ellis [1965] at higher frequencies also show dependence on the position of Io, although at the lower frequencies this becomes much less pronounced.

### c. Correlation With Solar Activity

The number of bursts is observed to vary from year to year. Carr et al., [1961] found an inverse correlation with solar activity in the period near the solar maximum years 1957-1960. However, from 1961 to 1964, the number of bursts per year near 20 Mc/s decreased markedly, suggesting a positive correlation [McCulloch, private communication]. There have also been reports of a short-term positive correlation with solar activity. Douglas [1960] found an increase on the days following solar bursts, although he stated that the effect was not statistically significant. Warwick, using only days when the Jupiter emission was observed above 30 Mc/s, showed that there is a pronounced clustering of bursts on the day of, and 1 or 2 days after, solar continuum events.

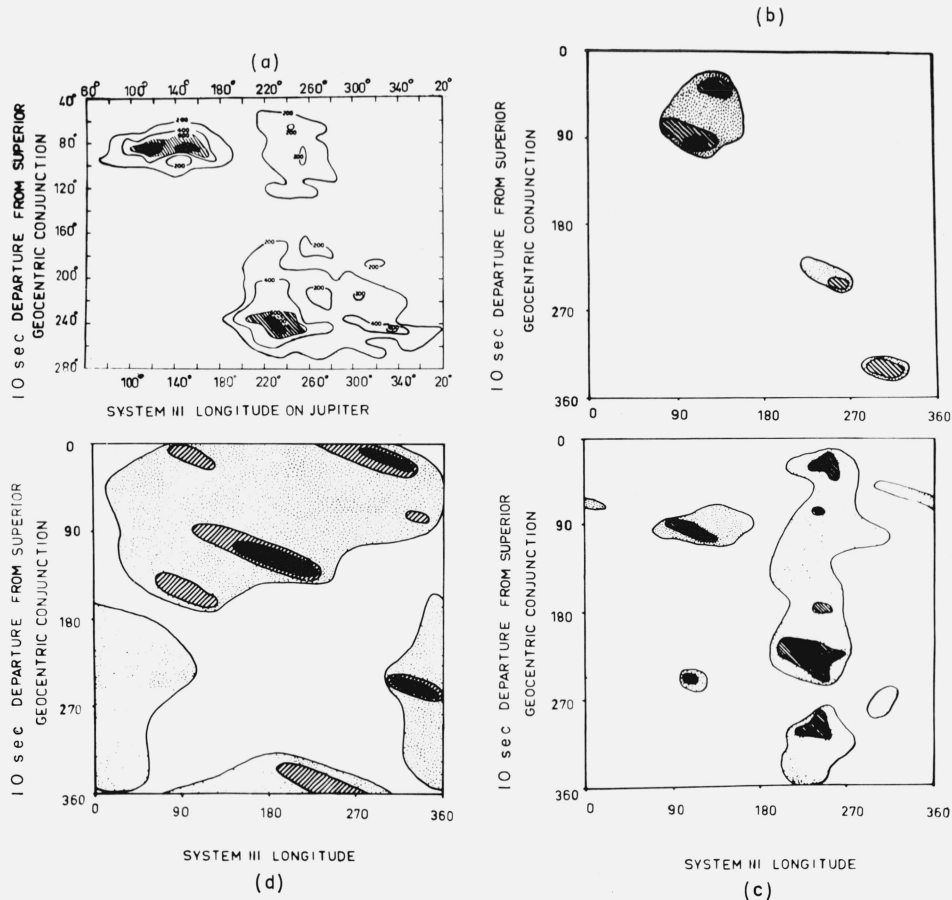


FIGURE 6. Variation of intensity of the radiation with position of satellite Io and System III longitude.

- (a) Frequency > 30 Mc/s [Bigg, 1964].
- (b) 28 Mc/s
- (c) 24.5 Mc/s [McCulloch and Ellis, 1965].
- (d) 4.7 Mc/s

### 2.3. Polarization

The polarization of the radiation was first studied by Franklin and Burke [1958] and by Carr et al., [1961]. Both groups found that most of the noise bursts observed at 22 Mc/s were right-handed in elliptical polarization (looking in the direction of propagation). Observations by Gardner and Shain [1958] showed similar polarization at 19.6 Mc/s. As the RH polarization had been observed at stations in both the Northern and Southern Hemispheres, it was concluded that this polarization was a property of Jupiter and not of the terrestrial ionosphere. During 1961 a few observations by Barrow [1962] at 18.3 Mc/s and 24 Mc/s suggested that a smaller proportion of RH bursts were to be found at 18.3 Mc/s than at 24 Mc/s. LH bursts were observed at 16 Mc/s by Barrow [1963]. Sherrill and Castles [1963], using a system which could be tuned to successive frequencies in the range 15 to 24 Mc/s, found a steady decrease in the portion of RH bursts with decreasing frequency. Dowden [1963b], working at 10 Mc/s, found that bursts of both RH and LH polarization were observed. In addition, Dowden was able to obtain for the first time sufficient observations to show how the polarization varied with the rotation of Jupiter (fig. 7). Dowden's results showed that the RH bursts were associated with the peaks in the occurrence rate between  $150^\circ$  and  $300^\circ$ , while the LH bursts occurred mainly between  $300^\circ$  and  $150^\circ$  longitude.

### 2.4. Ionospheric Effects

Gardner and Shain [1958] found considerable differences in the time variations of the radiation at sites 25 km apart. Subsequent investigations have been made over baselines of 150 m and 1000 km [Ellis and McCulloch, unpublished data; McCulloch and Slee, unpublished data], and by Douglas and

Smith [1961] over 15-km to 100-km baselines. These observations combine to show that all degrees of correlation can be experienced. At times there is very little correlation, whole groups of bursts being observed at one site and not at another, even with a baseline of 150 m (fig. 8). On the other occasions there can be essentially perfect correlation even with bursts as short as  $10^{-2}$  sec [Douglas and Smith, 1961]. Slee and Higgins [1964], using a phase-switching interferometer at 19.7 Mc/s with a baseline of 30 km, found on many occasions that good interferometric patterns could be obtained, implying that the actual radio-frequency waveform may be well correlated at this spacing. These observations are important in that they show that, even in spite of these ionospheric effects, high angular resolution measurements may be made and some estimate of the source sizes obtained. From their results they deduced that the source size was less than 19 sec of arc. All of the results of spaced observations are consistent with the assumption that the radiations are in the form of bursts with durations greater than approximately  $10^{-2}$  sec, and that in passing through the terrestrial ionosphere the bursts may at times be severely modulated by ionospheric irregularities.

## 3. Theories

### 3.1. General

The observed elliptical polarization points to an origin for the radiation in the acceleration of electrons in magnetic fields, and recent theories have all been based on radiation by electron streams traveling through a general Jupiter field. The existence of such a field has been suggested by the quite independent observations of microwave radio emissions from Jupiter.

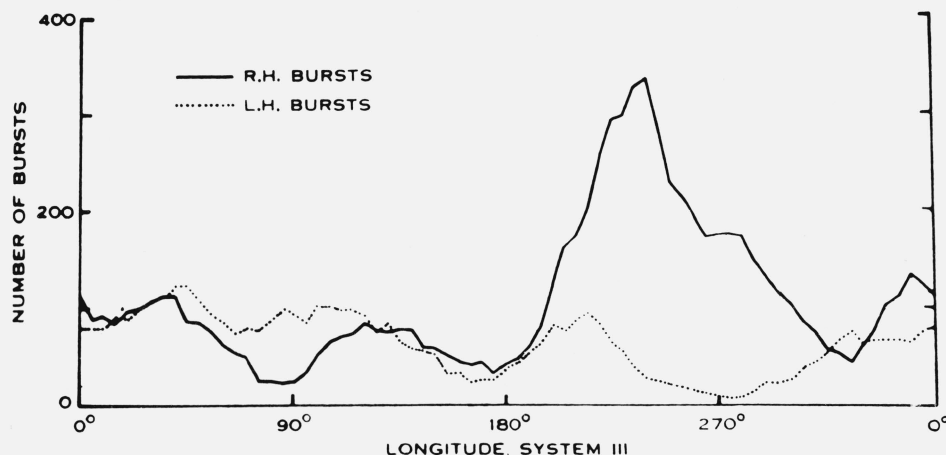


FIGURE 7. Variation of axial ratio of the polarization ellipses of the bursts with System III longitude at 10.1 Mc/s [Dowden, 1963b].

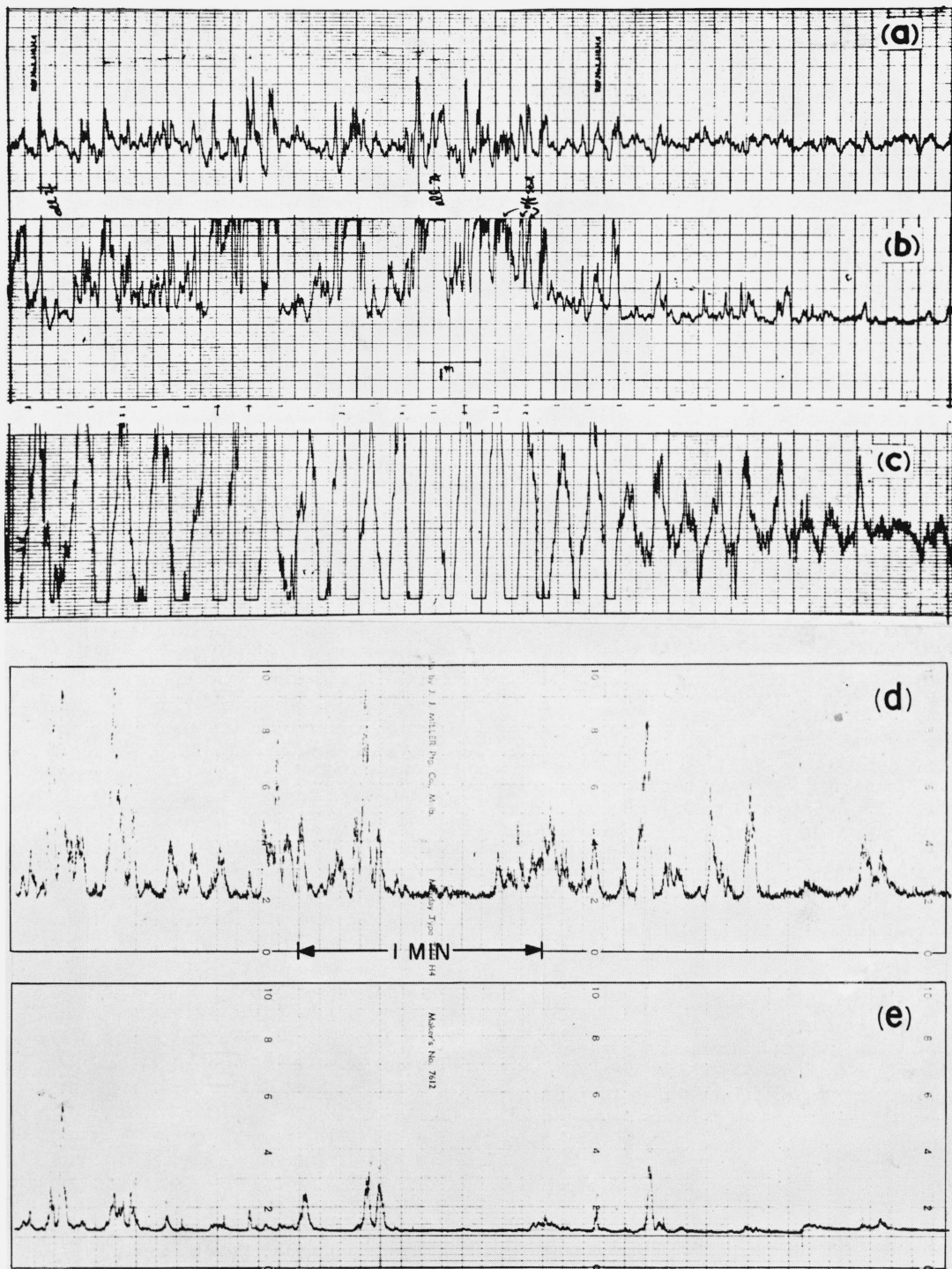


FIGURE 8. Spaced observation of bursts showing (a), (b), and (c), good correlation with spacing of 30 km [Slee and Higgins, 1964]. (d), poor correlation with spacing of 150 m [Ellis and McCulloch, unpublished data].

In order to discuss the different theories it is convenient at this point to review other probable characteristics of the environment in which the radiation is to be produced. The variation of the intensity and the polarization of the decimetric radiation with rota-

tion of the planet indicates that the North magnetic pole is in the vicinity of  $180^\circ$  System III and that the dipole axis is inclined at approximately  $10^\circ$  with respect to the rotation axis. The region in which this radiation is generated extends at least 2 Jupiter radii from the

planet in the equatorial plane and somewhat less along the axis. No information on the likely polar strength of the magnetic field is provided by these observations. However, if the frequency of the decametric radiation is taken to be somewhere near the electron cyclotron frequency, the polar field intensity cannot be less than about 15 G.

The solar flux in the upper atmosphere of Jupiter is likely to produce an ionosphere whose density has been estimated to be in the range of  $10^6$  to  $10^7$  electrons  $\text{cm}^{-3}$  [Field, 1959; Rishbeth, 1959]. Some spreading of this ionospheric plasma into the surrounding magnetosphere might be expected [Ellis, 1962]. Angerami and Thomas [1964] have shown that an ionosphere acts as a source region for the cold magnetospheric plasma, the density distribution in the magnetosphere being determined by the exchange of ions and electrons between the two regions along the magnetic field lines. For a fully ionized hydrogen atmosphere they give the density variation along a field line as

$$N = N_0 e^{-Z/2H}, \quad (1)$$

where  $H$  is the scale height,  $N_0$  is the density at the reference level in the ionosphere on the same field line, and  $Z$  is the potential height in the field.

For an isothermal atmosphere,

$$Z = r_0 \left( \left( 1 - \frac{\cos^2 \lambda_0}{\cos^2 \lambda} \right) + \frac{\Omega_r^2 r_0}{2g_0} \left( \cos^2 \lambda_0 - \frac{\cos^6 \lambda}{\cos^4 \lambda_0} \right) \right), \quad (2)$$

where  $r_0$ ,  $r$  are the radii of the reference level and the field point respectively,  $\Omega_r$  is the angular velocity,  $g_0$  is the gravitational constant at  $r_0$ ,  $\lambda$  is the latitude of the field point, and  $\lambda_0$  is the latitude of the reference point. We note at this stage that a relatively cold ionized magnetospheric plasma may be taken to be a consequence of the existence of an ionosphere.

In the terrestrial magnetosphere, electron streams of the type postulated to account for the Jupiter radiations arise in the vicinity of the magnetopause following the arrival of solar material [Ellis, 1957, 1959; Jokipii and Davis, 1964; Fan et al., 1964; Scarf et al., 1965]. The very-low-frequency electromagnetic radiations from the terrestrial streams have been used to determine their energy distribution, pitch distribution, and location [Dowden, 1963a]. It has been found that in general the electron momenta have a delta-

function distribution with  $\frac{\delta p}{p} \sim 1$  percent, and that they travel along field lines passing near the magnetopause. The electron energies are observed to be in the range 20 to 150 keV.

In the case of Jupiter, the radial distance of the magnetopause has been estimated by Ellis [1963] and Carr et al., [1964] on a basis of equality between the energy density of the field and the relative kinetic energy density of the interplanetary material. For a 15-G polar field and an interplanetary density of 1 proton  $\text{cm}^{-3}$ , Ellis finds the radius of the magnetopause to be  $35 R_J$ , and the field lines along which the electron streams might be expected to travel would have plane-

tary magnetic latitudes near  $80^\circ$ . It should be pointed out that if the rapid rotation of Jupiter is taken into account the radius of the outer boundary may be found to be much smaller, although it is likely to be greater than  $6 R_J$ .

Summarizing the probable properties of the environment, we have

(a) A general Jupiter magnetic field with a dipole axis inclined  $10^\circ$  with respect to the rotation axis.

(b) A polar magnetic field intensity of 15 G.

(c) An ionosphere with maximum electron density between  $10^6$  and  $10^7 \text{ cm}^{-3}$ .

(d) An ionized magnetospheric plasma in which the density distribution is determined by the distribution of density in the ionosphere, the appropriate scale height, and the gravitational and centrifugal forces acting on the ions.

(e) A magnetopause less than some 35 radii distant from the planet in the equatorial plane.

(f) Non-Maxwellian, almost mono-energetic, electron streams traveling down the field lines and originating near the magnetopause.

### 3.2. Theories

Warwick [1961] has proposed that the radiations are produced by a Cerenkov instability in the ionospheric plasma initiated by the precipitation of the electron stream into the ionosphere. The emission is taken to occur slightly below the local plasma cyclotron frequency, and the radiation to be beamed in the direction of motion of the particles, that is, inwards towards the planet. He supposed that the radiation is reflected either from dense layers of the ionosphere or from the surface of the planet, and that only for suitable orientations of the magnetic field and the surface of the planet will the reflected radiation be received at the earth.

Warwick supposed the field to contain only a dipole component with the dipole tilted  $9^\circ$  to the rotational axis. It was assumed that electrons are precipitated from the main radiation belt at 2 to 3 Jovian radii. Warwick assumed that the radiation generated by the electrons is confined within  $\pm 10^\circ$  of the field lines. Then for a number of trial assumptions concerning the location of the dipole with the planet, he computed the geometry of the reflections which reach the earth. For each of the rays reaching the earth, the relative intensity of the magnetic field in the generating region is deduced and possible longitude spectral profiles constructed.

He showed that profiles similar to the observed ones required that the dipole be located:

1. Near the axis of rotation but well away from the equatorial plane.

2. South of the equatorial plane and towards the earth when the central meridian longitude is  $200^\circ$ .

3. Displaced slightly from the  $\text{III} = 200^\circ$  plane to achieve the small asymmetry of the spectra about  $\text{III} = 200^\circ$ .

This model explains the two major sources of the decametric bursts above 20 Mc/s and their frequency drifts.



However, Warwick's theory has several unsatisfactory features, relating mainly to the proposed radiation mechanism, but also to the necessity for a highly asymmetric dipole position. Cerenkov radiation is in general not emitted in the direction of particle motion. Also, in the frequency region just below the plasma cyclotron frequency, the refractive index of the plasma will be high and substantial refraction of the ray will occur on emergence into free space. This refraction will not only change the mean direction of the ray but will also cause it to spread over a large cone. A parallel case is the emergence of whistlers below the terrestrial ionosphere. Finally, as the wave travels outwards the decrease in the planetary magnetic field and the plasma cyclotron frequency will require it to pass through a region where the wave frequency is equal to the cyclotron frequency. For the wave to escape without high attenuation, this region must have essentially zero plasma density. Since it has been assumed that in the generating region the wave frequency is only slightly less than the cyclotron frequency, the attenuating region will not be far above the ionosphere and it would seem to be hard to justify zero density for it.

Hirschfield and Bekefi [1963] and Field [1963] have proposed that the radiation is not Cerenkov radiation from the ambient plasma, but cyclotron radiation emitted by the electron stream itself. They have assumed that the radiation is generated in the magnetosphere in a region of zero plasma density and have shown that the process can produce radiation intensities similar to those observed. However, no detailed attempt to account for the other properties of the radiations was made.

The most comprehensive theory so far proposed is that of Ellis [1962, 1963] and Ellis and McCulloch [1963], who also suggested that the radiation is caused by cyclotron radiation from electron streams, but in the more general situation of a stream traveling through an ambient magnetospheric plasma. They examined the likely properties of cyclotron radiation generated by electron streams in the Jupiter environment and were able to show that most of the observations could be accounted for, providing only that the Jupiter magnetosphere and magnetic-field configuration are generally similar to those of the Earth. Comparison between the theory and the observations further permitted the estimation of the density of the magnetospheric plasma as well as the distribution of the magnetic field. We consider the development of this theory in more detail.

## 4. Doppler Cyclotron Theory

### 4.1. Electron Stream Radiation

In the presence of a magnetic field, a stream traveling through a plasma may be unstable with respect to radiative processes; that is, it may have a negative absorption coefficient, and radiation passing through the stream will be amplified, while electromagnetic disturbances within it will grow in time. In general,

there are at least four different instabilities with characteristic frequencies determined by the Doppler equation,

$$\omega = CK\beta \cos \phi \cos \theta + \Omega(1 - \beta^2)^{1/2}, \quad (3)$$

where  $K$  is the wave number equaling  $\frac{\eta\omega}{C}$ ,  $\Omega$  is the electron cyclotron frequency,  $\theta$  the angle between the wave normal and the magnetic field vector, and  $\phi$  the pitch angle of the electrons.

This expression represents resonance between the characteristic frequency of the excited wave and the Doppler-shifted cyclotron frequency of the electrons in the stream. The multiple instabilities arise from the frequency dependence of the refractive index  $\eta$  of the stream-plasma system.

The two main frequency regions in which the instabilities occur are (a)  $\omega < \Omega$ , where the refractive index is greater than unity and the longitudinal particle speed is greater than the phase speed (superluminous instability), and (b) where  $\omega > \omega_X$ , the extraordinary mode cutoff frequency:

$$\omega_X = \left( \sqrt{\omega_0^2 + \frac{\Omega^2}{4}} + \frac{\Omega}{2} \right) > \Omega. \quad (4)$$

Radiation generated by the former instability is subject to the same high attenuation in escaping from a magnetosphere referred to earlier in connection with Cerenkov radiation. However, in the case of the second instability region, no such barrier exists. The refractive index is always less than unity, and would asymptotically approach unity as the wave traveled outwards through the magnetosphere. Since the particle speed is necessarily less than the phase speed, this instability is referred to as the subluminous instability of the stream-plasma system.

Its properties have been investigated by Zelezniakov [1960], Ginsburg et al., [1962] and Neufeld and Wright [1964]. These authors have shown that necessary conditions for subluminous instability are the existence of a component of electron velocity transverse to the magnetic field, and a momentum distribution characterized by a delta function  $(\delta(P_1 - P_{1_0}))$ ,  $P_{1_0} \neq 0$ .

### 4.2. Angular Distribution of the Radiation

The angular distribution of the radiated energy cannot yet be calculated in detail for the case of an electron stream traveling through a plasma. However, the Doppler equation (3) shows that the instability exists if the longitudinal component of the electron velocity is sufficient to Doppler shift the radiated frequency to a value greater than  $\omega_X$ . Where the longitudinal electron velocity is greater than the minimum, the Doppler equation can be satisfied for a limited range of wave-normal directions, and the radiation is confined to a cone about the magnetic field direction. In the case of radiation from a single electron, the flux density tends towards infinity for the limiting direction in the surface of the cone. This type of distri-

bution cannot be assumed for a stream, since the amplification factor and the radiation intensity in a given direction would depend on the stream geometry, and in particular on the total path length. However, the radiation is emitted into an ambient plasma with refractive index less than unity, and the final angular distribution of the radiation will in any case differ from the original one because of refraction. The effects of refraction in a similar situation have been studied by Papagiannis and Huguenin [1964]. They have shown that, even if the initial distribution within the medium is isotropic, the emerging radiation is in general confined mainly to the surface of a cone whose angular radius is given by Snell's law:

$$\sin \alpha_{\max} \sim \eta \sin \theta \quad (5)$$

( $\alpha_m$  measured with respect to magnetic field vector). This relation is exact if planes of constant refractive index are normal to the magnetic field direction, and for simplicity in the present analysis this is assumed to be the case. This assumption amounts to taking the density of the magnetospheric plasma source region in the Jupiter ionosphere to increase slightly with magnetic latitude in the polar region. This behavior is observed for the terrestrial ionosphere. Where the radiation is initially emitted downwards, it will be reflected near the level  $\omega = \omega_x$ . Since  $\omega \sim \omega_x$  at generation, reflection will be near the point of emission and the cone angle will still be given by (5).

To find  $\alpha_m$  it is necessary to solve graphically simultaneously the Doppler equation and the wave number equation,  $K = K(N\omega\theta H)$ , for given values of electron density  $N$ , magnetic field intensity  $H$ , particle pitch  $\phi$ , and velocity  $\beta$ , letting  $\theta$  vary. For each value of  $\theta$  the solutions for wave frequency  $\omega$  and refractive index are obtained and  $\alpha$  can be calculated. A maximum value of  $\alpha = \alpha_m$  is found which is a function of the assumed parameters  $H$ ,  $\phi$ ,  $\beta$ , and  $N$ .

For  $\alpha = \alpha_m$ ,  $\frac{d\alpha}{d\theta}$  is found to be zero and the radiated power  $\mathcal{W}(\alpha)$  reaches a maximum according to  $\mathcal{W}(\alpha) \sin \alpha d\alpha = \mathcal{W}(\theta) \sin \theta d\theta$ .

The Doppler equation may be rewritten

$$\sin \alpha_m = \left[ \eta^2 - \frac{1 - \sqrt{1 - \beta^2} Y}{\beta \cos \phi} \right]^{1/2}, \quad Y = \frac{\Omega}{\omega}; \quad (6)$$

and for electron energies in the range 10–100 keV, and  $Y \sim 1$ ,  $\alpha_m$  is seen to be only a weak function of the electron energy but a strong function of the pitch angle  $\phi$  and of the ratio of the cyclotron frequency to the plasma frequency  $\Omega/\omega_0$ . The quasi-independence of  $\alpha_m$  on energy is valuable since it makes it unnecessary to make any detailed assumptions about the electron energy.

The further development of the theory follows from a straight-forward analysis of the consequences of the radiation being emitted in conical shells whose angular radius depends on the foregoing parameters, taking

into account the inclination of the cone axes, that is, the magnetic field vector, to the line of sight towards the earth.

### 4.3. Probability Distribution

To obtain information about the rate of occurrence of bursts, it is necessary to insert some appropriate probability assumption. It is assumed that each burst is produced by a bunch of electrons within the stream and that bunches of all pitch angles occur with equal probability. The number of bunches  $dN$  with pitch angles in the range  $\phi$  to  $\phi + d\phi$  is then

$$dN = \sin \phi d\phi. \quad (7)$$

Within each bunch, the pitch distribution is assumed to be a delta function. It is further assumed that as the planet rotates, electron bunches may occur with equal probability in all magnetic longitudes. This is a reasonable assumption for electrons originating in the magnetopause but might need modification to allow for the Io correlations.

Equations (6) and (7) together provide a functional relationship between the number of bunches traveling along a particular field line whose radiation is observable at a particular frequency and at angle  $\alpha_m$  with respect to the field-line direction at the point of emission. If this coordinate system is transformed to one based on magnetic latitude  $\lambda$  and longitude, and integration is carried out with respect to pitch angle and magnetic longitude, then the number of bunches  $N_\lambda$  whose radiation may be observed in a given magnetic latitude interval  $d\lambda$  is obtained. As the planet rotates, the observer's magnetic latitude changes by approximately  $\pm 10^\circ$ , and the change in the probability of observing bursts may then be taken from the curves for  $N = N(\lambda)$ . If it is assumed that the electrons are confined to field lines of a single latitude, the longitude profiles obtained in this way have a more rectangular shape than those observed. To obtain better agreement, the further assumption was introduced that the electron-stream field lines extended over a small range of latitudes. Taking into account the calculated magnetopause boundary at  $35 R_J$ , the probability of occurrence of electron streams was assumed to increase linearly with magnetic latitude from  $\lambda = 75^\circ$  to  $\lambda = 80^\circ$  and to be zero for  $\lambda < 75^\circ$ . This assumption is not an important one and was made only to allow the theory to match more accurately the observed profiles.

The calculated probability of observing bursts in different magnetic latitudes near the magnetic equator is then as shown in figures 9a and 9b. For a simple dipole magnetic field with the magnetic axis inclined to the rotation axis, the probability of observation at the Earth will obviously change in a quasi-sinusoidal way with rotation, with maxima in the longitudes of the poles. However, only in the average-power data at 4.7 Mc/s is such variation actually observed, and to account for the additional or anomalous maxima at higher frequencies it is necessary to introduce

some modification to the simple model considered so far. Such modification may obviously be in the form of a deviation of the magnetic dip angle from that of a dipole in the appropriate latitudes and longitudes. That is, if the cone axes are inclined more towards the equator the probability of observing bursts at the Earth will be greater. An equally valid alternative modification would of course be to take the cone angles  $\alpha_m$  to be larger for these longitudes. Such larger cone angles could result from a changed pitch-angle distribution or, less effectively, from higher energy particles in these longitudes. However, in any case, some anomalous magnetic field distortion appears necessary in the Northern Hemisphere to account for the asymmetry in the Io-correlated bursts with respect to the two magnetic poles.

If the amount of a dip-angle deviation is  $\delta$  in the plane of the magnetic meridian at a given height for which the ratio  $\Omega/\omega_0$  is constant, then the effect is to change the latitude datum of the corresponding probability curve in figure 9 by an amount equal to  $\delta$ . It may be seen from figure 9 that, with the assumed model, a latitude shift of the probability curve by a few degrees can produce a considerable change in the observed probability of occurrence.

The probability or power maxima which are associated with the poles may be identified from figure 6. There are four distinguishable maxima at  $130^\circ$ ,  $175^\circ$ ,  $240^\circ$ , and  $330^\circ$  longitude respectively, and it might be expected that those at  $175^\circ$  and  $330^\circ$  correspond with the poles if these latter are taken to be at  $180^\circ$  and  $360^\circ$ . Also, the amplitudes of these two maxima decrease rapidly with wave frequency, while the amplitudes of the others increase in the frequency range from 5 to 20 Mc/s (fig. 5). Now any magnetic anomalies would normally increase rapidly in their effects with decreasing radial distance, that is, with increasing wave frequency, while, conversely, the magnetic field would become more like that of a dipole at greater distances. This provides a second criterion for selecting the polar and anomalous maxima, and again it is found from figure 5 that the former are those at  $175^\circ$  and  $330^\circ$ . If the polar maxima can be identified, then the variation in the electron density with height may be estimated.

For each wave frequency the value  $\Omega$  is known, very nearly, and the expected variation in the probability of occurrence for different values of  $\Omega/\omega_0$  can be computed. Comparison of the calculated probability curves with those observed gives  $\Omega/\omega_0$  and hence  $\omega_0$ . In addition, the height for which this value of  $\omega_0$ , and consequently the electron density, is appropriate, is obtained from the variation of  $\Omega$  with height. If the electron density is specified in this way, the dip anomalies needed to account for the anomalous occurrence maxima may be obtained easily from figure 9. The expected variation of probability and power with longitude, including anomalies, may then be computed. The calculated electron densities are shown in figure 10, the dip anomalies in figure 11, and the resulting expected probability curves in figure 12.

It is seen that the theoretical curves agree well

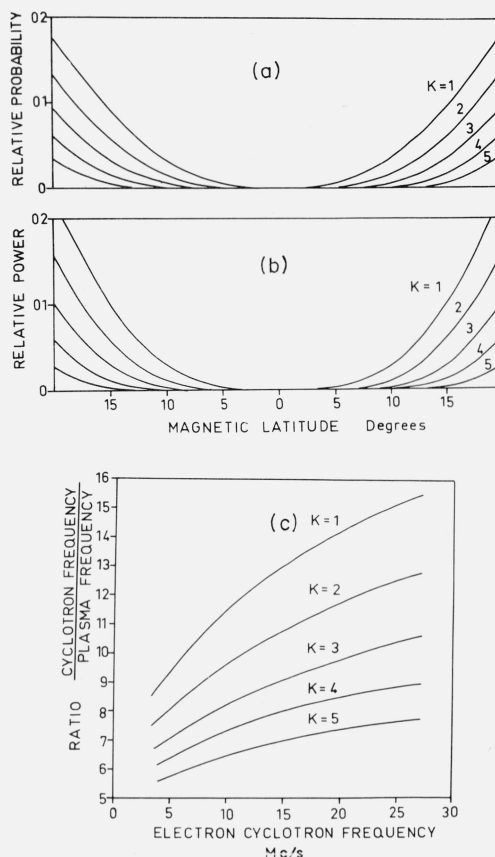


FIGURE 9a. Calculated variation of the probability of observation of radiation bursts with magnetic latitude.

The probability of occurrence of electron streams is assumed to increase linearly with magnetic latitude for field-line latitudes greater than  $75^\circ$ . Electron energies 30–60 keV.

FIGURE 9b. Calculated variation in average power of observed bursts with magnetic latitude.

FIGURE 9c. Relation between parameter K in (a) and (b) and plasma and cyclotron frequencies.

with those observed for all frequencies in their general shape, although accurate matching between the properties of the model and the observations must await more complete data. However, it should be noted that, since in the cyclotron theory the observability of a burst depends on the inclination of the field line at the point of emission, any observed pattern in the occurrence of bursts may be accounted for by slight suitable adjustments of the magnetic field configuration of the type discussed here. This adjustment need not be confined, of course, to local variations in the dip angle, but may include the moving of the dipole axis to an asymmetric position with respect to the rotation axis, as suggested by Warwick [1963a].

#### 4.4. Polarization

The distribution of the polarization of the bursts is contained in the foregoing theory since the axial ratio

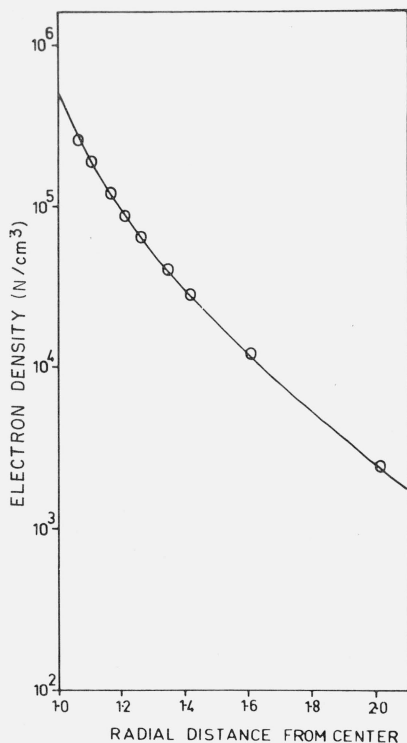


FIGURE 10. Calculated variation of electron density with height along-high-latitude field lines.

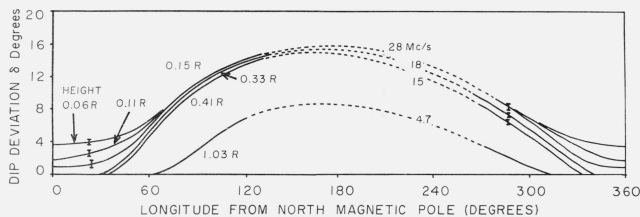


FIGURE 11. Calculated variation in the deviation of the dip angle from that of a dipole in magnetic latitudes  $75^\circ$  to  $80^\circ$  as a function of longitude. The variation needed to account for the longitude probability profiles at different frequencies is indicated in the diagram.

$A$  of the polarization ellipse will depend mainly on the angle of the emission cone. That is,

$$A = \pm \cos \alpha_m. \quad (8)$$

Since the cone angle is a function of the pitch angle, which is itself a function of the number of bunches, the axial ratio is necessarily a function of the bunch number. That is,

$$\alpha = \alpha(\phi) \quad (9)$$

$$dN = dN(\phi) \quad (10)$$

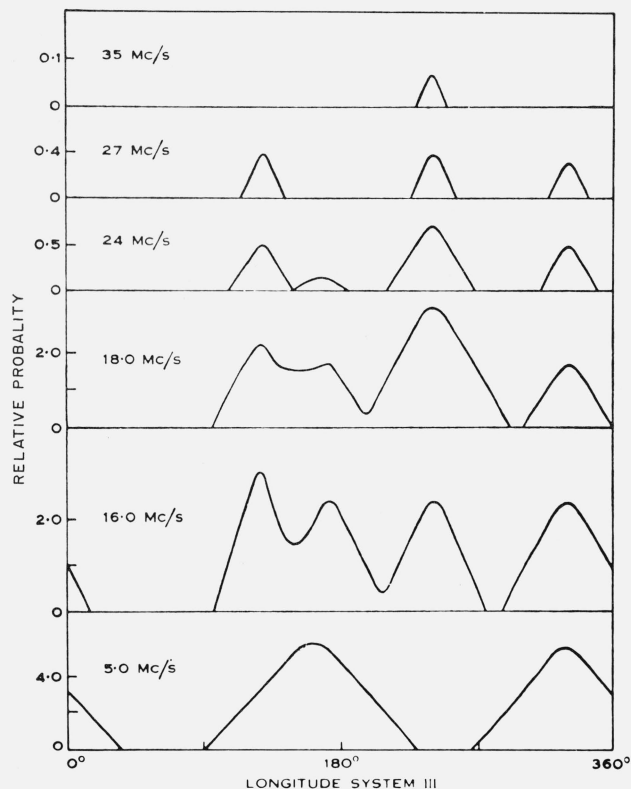


FIGURE 12. Calculated variation of probability with longitude.

or, integrating over pitch angle, latitude, and longitude; the summed axial ratio is obtained as a function of the total number of the observable bunches:

$$\Sigma A = \Sigma A(N). \quad (11)$$

The particular function relationship is determined essentially by the form of the Doppler equation and the assumption of uniform probability of pitch angle, and is predicted by the theory to be

$$\Sigma A \propto N^{1.05}. \quad (12)$$

Good agreement is actually observed on this point. Sherrill [1965] and Dowden [1963b] have both found that the summed axial ratio of the observed polarization ellipses is a logarithmic function of the number of bursts with exponent 1.05 and 1.10 respectively (fig. 13).

The distribution of axial ratios obtained from the theory is shown in figure 14. Again a distribution of the observed type is found. Figure 15 shows the expected variation in mean axial ratio with the latitude of the electron stream.

#### 4.5. Integrated Power

If the power emitted by the electron is a function of the pitch angle, then a functional relationship can easily be established between the integrated power and



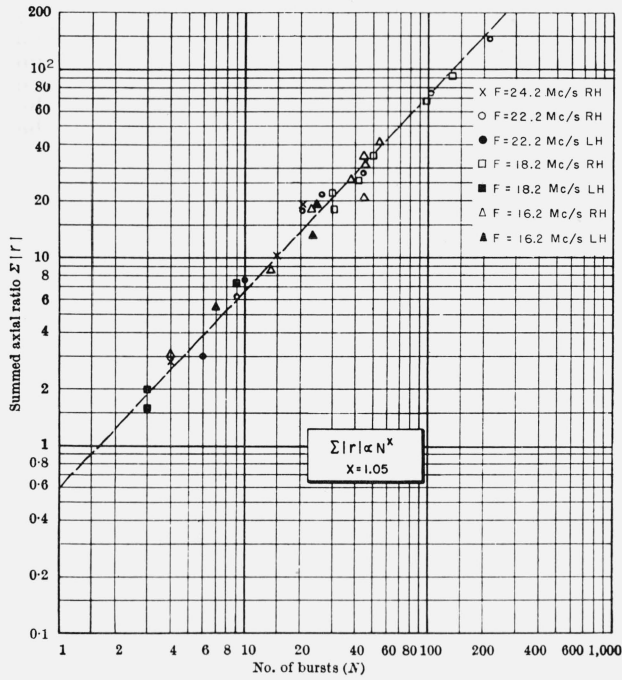


FIGURE 13. Theoretical variation of summed axial ratio with number of bursts (broken line), and observations by Sherrill [1965].

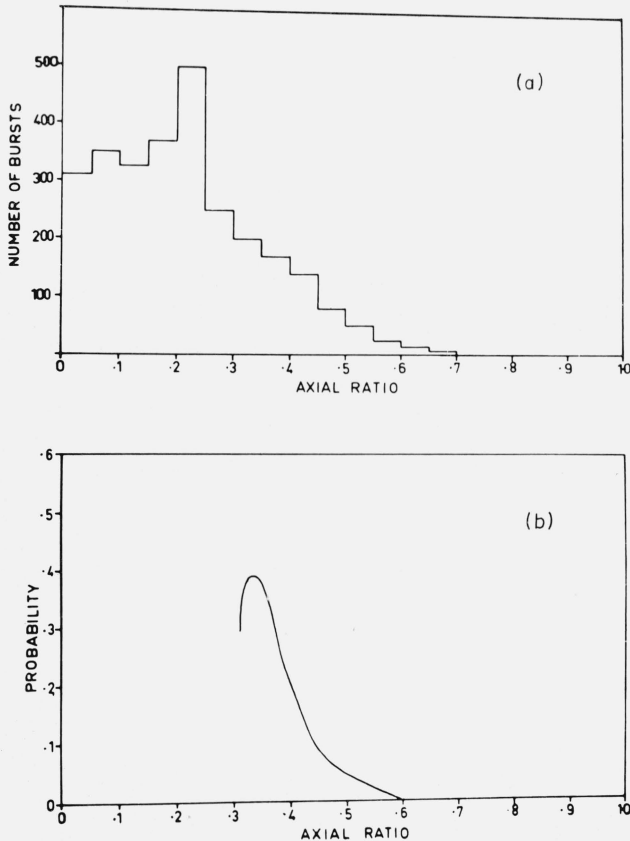


FIGURE 14. Theoretical and observed distribution of axial ratios at 10 Mc/s, after Dowden [1963b].

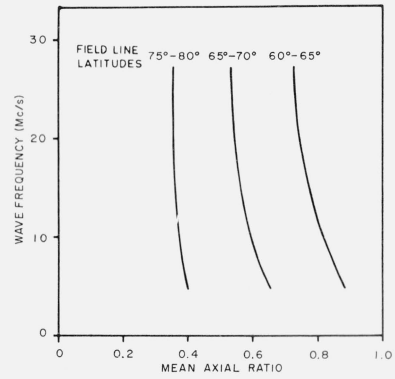


FIGURE 15. Calculated variation of mean axial ratio with latitude of electron stream.

the total number of bursts. For a single electron, the radiated power  $W_e \propto \sin^2 \phi$ , and if this can be taken to be characteristic of the radiation of bunches, then for  $dN$  bunches the power will be

$$W = W_b dN = W_b \sin^3 \phi d\phi \quad (13)$$

if radiation from single bunches  $W_b$  can be taken to add randomly. If interaction between bunches exists, this relation would need to be modified in the direction of stronger dependence on  $dN$ . With no interaction, the relation between the integrated power and the number of bursts is found to be

$$W_1 \propto N^{1.3}. \quad (14)$$

That is, where the bursts are more numerous they are also stronger. Dowden [1963b] found at 10.1 Mc/s that such a functional relationship existed, but that the exponent was 1.51. This discrepancy could be caused by the use of an incorrect pitch-angle function for the radiated power or by failing to take account of superimposed bursts in counting the number.

The variation of flux density with frequency calculated using the foregoing model is shown in figure 16.

#### 4.6. Spectral Variations

Unlike the observations and the expected properties of the radiation so far considered, the spectral observations give information about individual occurrences rather than their time averages, and it is necessary to discuss the distribution of the radiation from electron bunches traveling down a single field line.

Different wave frequencies will be emitted at different heights for which the direction of the magnetic vector and the ratio  $\Omega/\omega_0$  are determined from the characteristics of the model and the deduced electron-density distribution. The angle of the radiation cone  $\alpha_m$  will therefore vary with frequency, and as the latitude and longitude of the observer change with the rotation of the planet, the observed frequency will change with time, provided that the stream of electron bunches lasts for the duration of the observations.

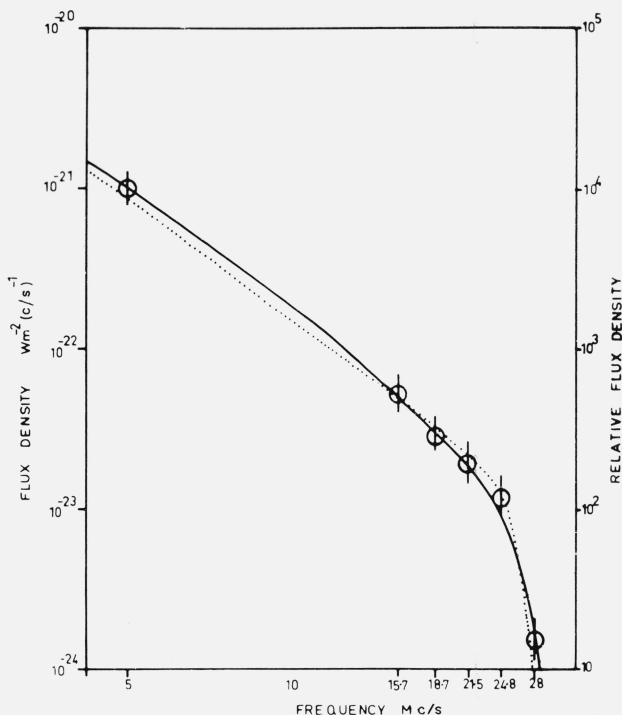


FIGURE 16. Calculated spectrum (dotted line) and observed spectrum (solid line).

The frequency-time curves calculated with electron streams in different latitudes are illustrated in figure 17a, where the electron streams are taken to occur simultaneously over a range of longitudes; then a broad, filled-in frequency-time spectrogram of the type shown in figure 15b will result from the rotation of the planet. If the radiation cone from an individual bunch is not of negligible angular thickness as has been assumed, then within the slowly varying frequency-time function produced by the rotation of the planet much more rapid variations could be observed. These would be produced by the change in radiated frequency with time as the individual bunch travels down or up the field lines [see Ellis, 1962]. The rate of change of frequency is given by

$$\frac{d\omega}{dt} \sim \frac{d\Omega}{dt} = -3 \frac{\Omega}{r} \frac{dr}{dt} \sim -3 \frac{\Omega}{r} V_{11}, \quad (15)$$

where  $V_{11}$  is the longitudinal velocity of the electrons and  $\Omega_0$  is the cyclotron frequency at the planet. Observation and measurement of the fine frequency-time structure of the bursts would hence be expected to give information about the velocity of the electrons. With the range of electron energies assumed in the

preceding section of 30–60 keV,  $\frac{df}{dt}$  would be in the range 30 to 50 Mc/s/sec. Figure 17d shows the expected appearance of the fine structure.

Each of the narrow spectra shown in figure 15a corresponds to the emission from a succession of

electron bunches or an electron stream of constant pitch angle confined to a given field line and lasting for the duration of the spectrum. If the pitch angle of the electrons at a given height is not constant during the life of the emission, or if the cross-sectional area of the stream is not infinitesimal, then the spectrum will be broadened. Hence it is possible by inspection of the observed spectra to set limits on the area of the stream and consequently on the angular size of the source as seen from the earth.

Some of the spectra observed, for example, have a longitude width at a single frequency of only  $5^\circ$ . Even if we assumed that the pitch angles were constant, and that the electron stream were confined to a single latitude, this implies that the longitude spread is only  $5^\circ$ . Relaxation of these restrictions would lead to a smaller value. The observed spectra therefore indicate that the sources of the radiation may be very small. The more diffuse spectra shown in figure 1 can be accounted for by larger sources or variation in the pitch angles.

## 5. Discussion

### 5.1. Properties of the Jupiter Magnetosphere

The variation of electron density deduced from the theory shows a logarithmic decrease with height as might be expected. However, the scale height of 2000 km obtained using (1) is high compared with the scale height in the terrestrial magnetosphere, and would imply a temperature in the lower Jupiter magnetosphere of about 7500 °K (Earth = 1000 to 2000 °K). On the other hand, some heating of the magnetosphere might be expected from the existence of satellites orbiting through it.

The proposed magnetosphere would be unusual compared with that of the Earth because of the high rotational velocity. Whereas for the Earth modification to the electron density-height profile by centrifugal force is only small, and is in any case significant only beyond 6 Earth radii, for Jupiter it would become important at 3 Jupiter radii and could conceivably result in an increase in the density at greater distances depending on the temperature distribution. The strong effects due to gravity and rotation would appear, from (2), to lead to surfaces of constant density being axially symmetric about the rotation axis, and hence asymmetric with respect to the dipole axis. This could have important consequences in the propagation of hydromagnetic waves in the magnetosphere, as will be discussed later. A general analysis of the whole question of the Jupiter magnetosphere is desirable along the lines initiated by Angerami and Thomas [1964] for the terrestrial magnetosphere.

The magnetic anomalies proposed do not appear to be excessive when compared with the similar anomalies in the geomagnetic field. The deviations of the magnetic dip from the dipole configuration at corresponding heights and at similar geomagnetic latitudes are of at least the magnitude found for Jupiter.

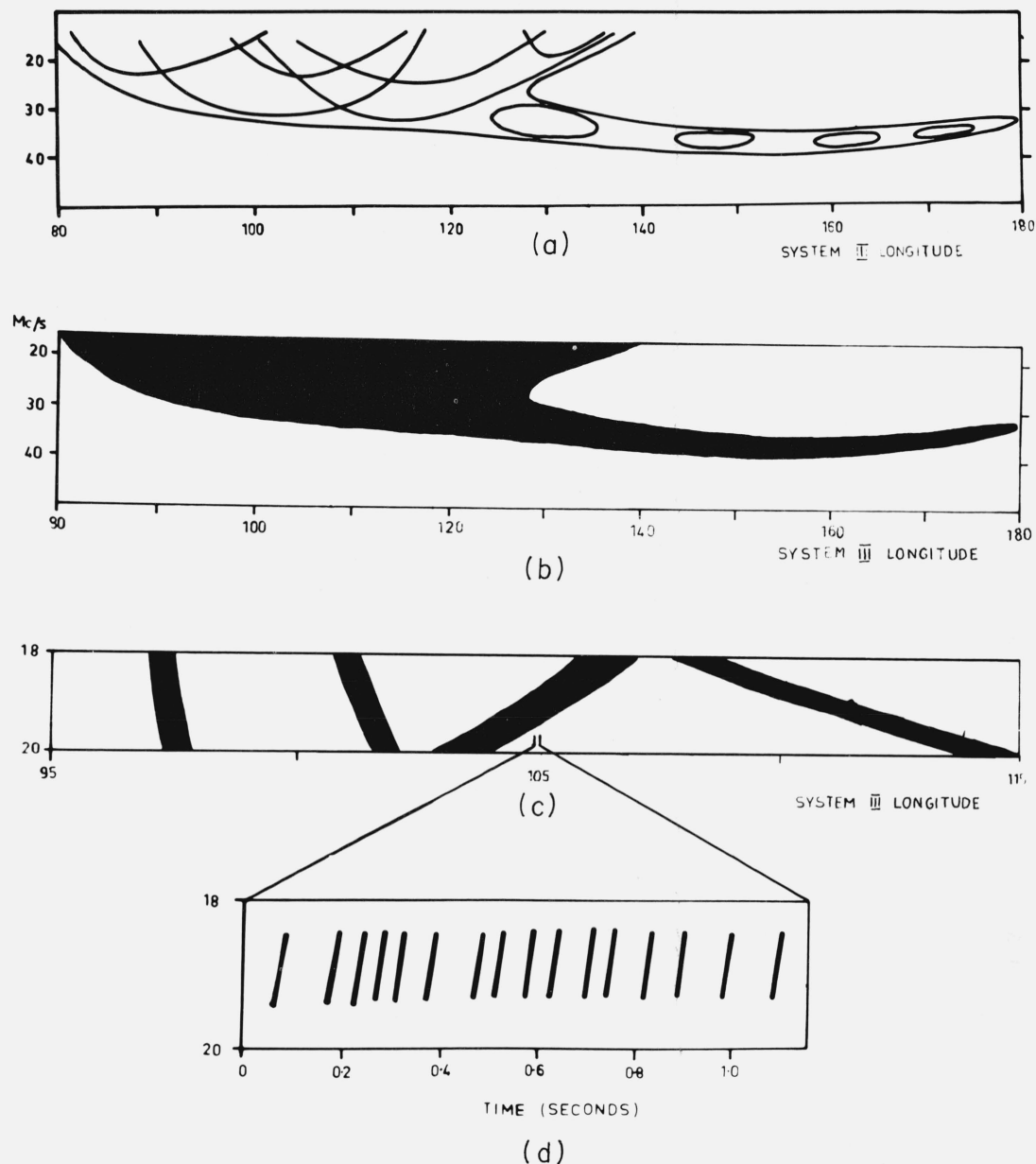


FIGURE 17. *Calculated frequency-time variation above 18 Mc/s.*

- (a) Individual lines show  $f-t$  variation from electron stream in a particular longitude and produced by rotation of Jupiter.  
 (b) Integrated  $f-t$  variation from electron streams occurring simultaneously over a range of longitudes.  
 (c) Calculated  $f-t$  variation in the 18–20 Mc/s frequency range used by Riihimaa [1964a]; see figure 1c. Electron streams in particular longitudes.  
 (d) Calculated fine structure due to individual bunches within a stream. For bunches traveling downwards the frequency increases with time, while for bunches observed after they have been reflected at their mirror points the frequency decreases with time. With electron velocity  $0.2C$ , pitch  $45^\circ$ ,  
 $\left[\frac{d\omega}{dt}\right]_{\omega=20 \text{ Mc/s}} = 36 \text{ Mc/s/sec.}$

On the Earth they result essentially from the displacement of the magnetic dip poles from the geomagnetic poles.

The distribution of axial ratios provides information of the angular radii of the emission cones and hence of the field-line latitudes. These have been chosen

as  $75^\circ$  to  $80^\circ$  in the analysis reviewed here. However, better agreement with the axial ratio observation of Sherrill and Castles [1963] would be attained by somewhat lower latitudes with a maximum of about  $68^\circ$ . Information on the detailed distribution of the electron streams in latitude could be obtained by sufficiently accurate longitude-probability profiles.

## 5.2. Satellite Periodicities

Periodicities in the observability of the radiation associated with the orbital position of Io may be caused according to the theory if either the occurrence of electron streams or the momentum distribution of electrons within the streams is modified by Io, possibly via hydromagnetic or electromagnetic radiation from Io. It is well known from observations of the terrestrial magnetosphere that such radiation can stimulate the emission of coherent radiation by an existing but nonradiating particle stream. The evidence suggests that where the momentum distribution of the stream is insufficiently narrow to give a negative amplification coefficient, exposure to external radiation can lead to the initiation of general radiation from the stream [Helliwell, 1963; Cornwall, 1965]. To explain the Io correlation, preconditions would be first that Io generate the hydromagnetic or electromagnetic radiation and, second that the radiation propagate through the large difference in Jupiter longitude between the position of Io and the source region of the decametric radiation.

At the orbit of Io the extrapolated value of the electron density would be at least  $10^3 \text{ cm}^{-3}$  and possibly greater than  $10^4 \text{ cm}^{-3}$ , depending on the temperature distribution. That is, the Alfvén velocity would be between 2400 and 750 km/sec. The relative velocity of Io through the magnetosphere is 54 km/sec. However, the motion of Io is almost normal to the magnetic field and this produces a situation quite different from that for the motion of charged particles through a plasma where the guiding center motion of the particles is along the field. The velocity of phase propagation for hydromagnetic waves may be zero in the direction normal to the field, while for electromagnetic waves above the ion cyclotron frequency but below the electron cyclotron frequency, the phase velocity tends to zero in direction given by

$$\cos \theta = \frac{\omega}{\Omega}.$$

The velocity of Io will hence exceed the velocity of phase propagation in its direction of motion for all wave frequencies less than the electron cyclotron frequency, and the satellite will continuously excite Cerenkov shock waves in the surrounding medium. For hydromagnetic waves at less than the ion cyclotron frequency, the initial direction of ray propagation will be along the magnetic field.

To calculate the ray trajectories of these radiations, it would be necessary first to develop a detailed model of the Jupiter magnetosphere out to the orbit of Io. However, it may be noted in considering the question of propagation that, as a consequence of the leveling-off in the density variation with height implied by (2), there will be a minimum in the refractive index at a height of about  $1.5 R_J$ . A similar minimum exists in the terrestrial magnetosphere at about  $0.5 R_E$ . It has been shown by Dessler et al., [1960] that the trajectory of HM waves in the Earth's magnetosphere is strongly affected by the refractive index minimum. If an in-

coming HM wave is incident normally in the minimum region, then no bending of the path occurs. However, for a small but nonzero angle of incidence in longitude, a large horizontal component develops in the trajectory (fig. 18b), which then ends in a longitude quite different from that of its beginning.

For Jupiter, the magnetic meridian planes are inclined to the rotation-system meridian planes except in longitudes  $180^\circ$  and  $360^\circ$ . The sense of the inclination is that, between  $180^\circ$  and  $360^\circ$  in the Northern Hemisphere, the magnetic meridian planes are tilted in the direction of smaller System III longitude with the opposite tilt between  $000^\circ$  and  $180^\circ$ . A wave originating at the satellite in longitudes  $180^\circ$  to  $360^\circ$ , and traveling initially parallel to the magnetic field, will hence be refracted ahead of the satellite, while one originating in  $0^\circ$  to  $180^\circ$  will be refracted behind the satellite. To account for the Io correlation it would be necessary for the refraction to produce a longitude shift of approximately  $130^\circ$ . Ray paths of the type required are illustrated in figure 18a. Refraction

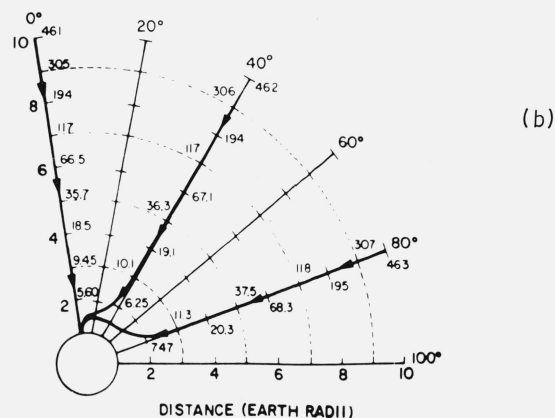
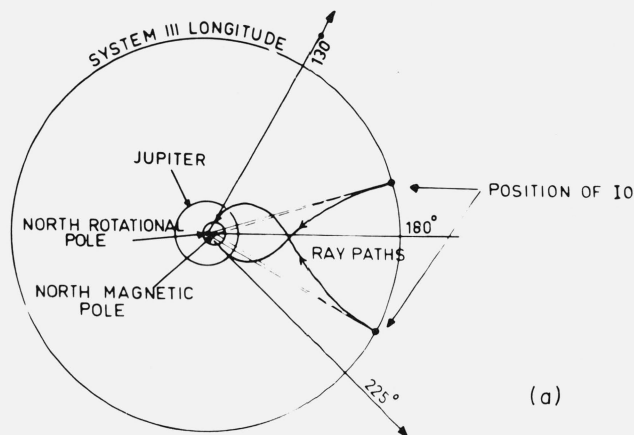


FIGURE 18a. Relative positions of Io and Jupiter for observation of radiation from longitudes 130 and 225°, System III. Possible ray paths of HM radiation are indicated.

FIGURE 18b. Ray paths of HM waves in the terrestrial magnetosphere [Dessler et al., 1960].



would appear to operate in the right sense, although quantitative evaluation is needed to properly assess this hypothesis.

If the HM waves propagate in this way, they may increase the probability of observing decametric radiation from electron streams in the region near the end of their ray trajectories through wave-particle interaction. Magnetic anomalies of the type illustrated in figure 11 are still required to give the observed variation of occurrence with System III longitude at the higher frequencies. However, where the proposed anomalies are small, as at the greater height of the 5-Mc/s radiation source, it might be expected on the HM hypothesis that longitude variations characteristic only of the position of Io and not of a combination of Io with magnetic anomalies might result. For example, with refraction as illustrated in figure 16a, a rapid change from forward refraction to backward refraction would occur when Io passed through longitude  $180^\circ$  where the rotation and dipole axes are coplanar. The intensity of HM illumination of the  $180^\circ$  region would hence be low with Io at  $180^\circ$  longitude, that is, at  $180^\circ$  from superior geocentric conjunction. It is interesting to note from figure 6d that at 4.7 Mc/s the integrated power of the radiation is low for this particular Io-Jupiter configuration.

## 6. Conclusions

The general observed properties of the Jupiter decametric radiations are now well established. However, this survey shows that important information is likely to be obtained from frequency-time spectra with higher frequency and time resolution than have so far been used. A time resolution of at least  $10^{-2}$  sec would appear to be necessary to show up the frequency structure of the shortest bursts.

The 30-km baseline interferometry studies of Slee and Higgins show that even at 20 Mc/s the ionosphere does not prevent observations with an angular resolution less than 20 sec of arc. If the technique could be developed further, the theoretical prediction of the small size of the radiation sources could be tested.

Further work on the data periodicities is needed, particularly with respect to the periods of other satellites and to solar activity.

On the theoretical side, although it appears that the properties of the emissions may adequately be explained on the basis of Doppler-shifted cyclotron radiation from electron streams, it should be emphasized that this theory is the only one which so far has been worked out in any detail. The other alternative theories may similarly prove able to offer a satisfactory account. Finally, the general theory of a rapidly rotating magnetosphere needs to be investigated in detail.

## 7. References

- Angerami, J. J., and J. O. Thomas (1964), Studies of planetary exospheres -I. The distribution of electrons and ions in the earth's exosphere, *J. Geophys. Res.* **69**, No. 21, 4537-4560.
- Barrow, C. H. (1962), Recent radio observations of Jupiter decametric wavelengths, *Astrophys. J.* **135**, 847-854.
- Barrow, C. H. (1963), Radiation from Jupiter, *Nature*, **197**, 580.
- Bigg, E. K. (1964), The influence of the satellite Io on Jupiter's decametric emission, *Nature* **203**, 1008-1010.
- Burke, B. F., and K. L. Franklin (1955), Radio emission from Jupiter, *Nature* **175**, 1074.
- Carr, T. D., A. G. Smith, H. Bollhagen, N. F. Six, and N. E. Chatterton (1961), Recent decameter-wavelength observations of Jupiter, Saturn, and Venus, *Astrophys. J.* **134**, 105-125.
- Carr, T. D., G. W. Brown, A. G. Smith, C. S. Higgins, H. Bollhagen, J. May, and J. Lery (1964), Spectral distribution of the decametric radiation of Jupiter in 1961, *Astrophys. J.* **140**, 778-795.
- Cornwall, J. M. (1965), Cyclotron instabilities and electromagnetic emission in the ULF and VLF frequency ranges, *J. Geophys. Res.* **70**, No. 1, 61-69.
- Dessler, A. J., W. E. Francis, and E. N. Parker (1960), Geomagnetic storm sudden-commencement rise lines, *J. Geophys. Res.* **65**, No. 9, 2715-2719.
- Douglas, J. N. (1960), A study of non-thermal radio emission from Jupiter, Ph. D. thesis, Yale University.
- Douglas, J. N., and A. J. Smith (1961), Presence and correlation of fine structure in Jovian decametric radiation, *Nature* **192**, 741.
- Dowden, R. L. (1963a), Method of measurement of electron energies and other data from spectrograms of VLF emissions, *Australian J. Phys.* **15**, 490-503.
- Dowden, R. L. (1963b), Polarization measurements of Jupiter radio bursts at 10.1 Mc/s, *Australian J. Phys.* **16**, 398-410.
- Ellis, G. R. A. (1957), Low frequency radio emission from aurorae, *J. Atmospheric Terrest. Phys.* **10**, 302-306.
- Ellis, G. R. A. (1959), Low frequency electromagnetic radiation associated with magnetic disturbances, *Planet. Space Sci.* **1**, No. 4, 253-258.
- Ellis, G. R. A. (1962), Cyclotron radiation from Jupiter, *Australian J. Phys.* **15**, 344-353.
- Ellis, G. R. A. (1963), The radio emissions of Jupiter and the density of the Jovian exosphere, *Australian J. Phys.* **16**, 74-81.
- Ellis, G. R. A., and P. M. McCulloch (1963), The decametric radio emissions of Jupiter, *Australian J. Phys.* **16**, 380-397.
- Fan, C. Y., G. Gloeckler, and J. A. Simpson (1964), Evidence for 30-keV electrons accelerated in the shock transition region beyond the earth's magnetospheric boundary, *Phys. Rev. Letters* **13**, 149-153.
- Field, G. B. (1959), The source of radiation from Jupiter at decimeter wavelengths, *J. Geophys. Res.* **64**, 1169-1177.
- Field, G. B. (1963), Jupiter's radio emission (private communication).
- Franklin, K. L., and B. F. Burke (1958), Radio observations of the planet Jupiter, *J. Geophys. Res.* **63**, 807-824.
- Gallet, R. M. (1957), The results of the observations of Jupiter's radio emissions on 18 and 29 Mc in 1956 and 1957, *IRE Trans. Ant. Prop.* **AP-5**, 327-328.
- Gallet, R. M. (1961), *The Solar System*, vol. 3, Planets and Satellites, ed. G. P. Kuiper and B. M. Middlehurst (Univ. of Chicago Press, Chicago).
- Gardner, F. F., and C. A. Shain (1958), Further observations of radio emission from the planet Jupiter, *Australian J. Phys.* **11**, 55-69.
- Ginzburg, V. L., V. V. Zheleznyakov, and V. Ya. Eidman (1962), The radiation of electromagnetic waves and the instability of electrons moving at super-light velocity in a medium, *Phil. Mag.* **7**, 451-458.
- Helliwell, R. A. (1963), Whistler-triggered periodic very-low-frequency emissions, *J. Geophys. Res.* **68**, 5387-5395.
- Hirschfeld, J. L., and G. Bekefi (1963), Decameter radiation from Jupiter, *Nature* **198**, 20.
- Jokipii, J. R., and L. Davis (1964), Acceleration of electrons near the earth's bow shock, *Phys. Rev. Letters* **13**, 739-741.
- Kraus, J. D. (1958), Planetary and solar emission at 11 meters wavelength, *Proc. IRE* **46**, 266-274.
- Morrison, B. L. (May 1, 1962), U.S. Naval Obs. Circ. No. 92.
- McCulloch, P. M., and G. R. A. Ellis (1965), Observations of Jupiter's decametric radiation, *Planet. Space Sci.* (to be published).
- Neufeld, J., and H. Wright (1964), Interaction of a plasma with a "helical" electron beam, *Phys. Rev.* **135**, A1175-A1189.
- Papagiannis, M. D., and G. R. Huguenin (1964), Ionospheric focusing in the presence of the earth's magnetic field, *J. Geophys. Res.* **69**, No. 7, 1307-1318.

- Riihimaa, J. J. (1964a), High resolution spectral observations of Jupiter's decametric radio emission, *Nature* **202**, 476-477.
- Riihimaa, J. J. (1964b), Observations of the fine structure of Jupiter's decametric radio emission, *Ann. Acad. Sci. Fennicae, Ser. A VI* **156**.
- Rishbeth, H. (1959), The ionosphere of Jupiter, *Australian J. Phys.* **12**, 466-468.
- Scarf, F. L., W. Bernstein, and R. W. Fredricks (1965), Electron acceleration and plasma instabilities in the transition region, *J. Geophys. Res.* **70**, No. 1, 9-20.
- Shain, C. A. (1956), 18.3 Mc/s radiation from Jupiter, *Australian J. Phys.* **9**, 61-73.
- Sherrill, W. M. (1965), Polarization of Jovian emission at decametric wavelengths, *Nature* **205**, 270-271.
- Sherrill, W. M., and M. P. Castles (1963), Survey of the polarization of Jovian radiation at decametric wavelengths, *Astrophys. J.* **138**, 587-598.
- Slee, O. B., and C. S. Higgins (1964), Long baseline interferometry of Jovian decametric radio bursts, *Nature* **197**, 781-782.
- Warwick, J. W. (1961), Theory of Jupiter's decametric radio emissions, *Ann. N. Y. Acad. Sci.* **95**, 39.
- Warwick, J. W. (1963a), Dynamic spectra of Jupiter's decametric emission, 1961, *Astrophys. J.* **137**, 41-60.
- Warwick, J. W. (1963b), Repeatability of Jupiter's decametric radio emissions, *Science* **140**, 814-816.
- Zelezniakov, V. V. (1960), The stability of a magnetoactive perturbations, *Radiophysica* **3**, 57.

## 8. Additional Related Reference

- Roberts, J. A. (1963), Radio emission from the planets, *Planet. Space Sci.* **11**, 221-259.

## Discussion Following Ellis's Paper

*J. W. Warwick:* Have you a deductive theory of Jupiter's magnetosphere?

*Answer:* Yes, the scale height is the sensitive parameter of the theory, and for Jupiter must correspond to 5000 °K instead of the 1000 °K of the Earth's magnetosphere.

*S. Silver:* Is there reason to suppose that there is a magnetosphere structure around Jupiter?

*Answer:* Yes. It depends on the temperature.

*C. Sagan:* What about Jupiter V, the innermost satellite?

*Answer:* There may be possible effects, depending on the electron density profile in the magnetosphere.

*J. A. Roberts:* The field lines intersecting Jupiter V may be too low in latitude to correspond to observable effects.

*C. Sagan:* Does the existence of a satellite atmosphere fit your theory?

*Answer:* Yes.

*I. Shapiro:* Does Io rotate fast enough to have its own field?

*Answer (by C. Sagan):* Maps of the Galilean satellites exist and show that they all rotate synchronously.

(Paper 69D12-583)

# Results of Recent Investigations of Jupiter's Decametric Radiation

T. D. Carr, S. Gulkis, A. G. Smith, J. May, G. R. Lebo, D. J. Kennedy, and H. Bollhagen

Department of Physics and Astronomy, University of Florida, Gainesville, Fla.

The activity of Jupiter's decametric radiation appears to be greatest between 5 and 10 Mc/s, but measurements made below 10 Mc/s are subject to large ionospheric errors. No significant change in rotation period has appeared since 1960. The effect of the satellite Io as reported by Bigg has been corroborated. Marked variations in axial ratio with System III longitude were observed, from which estimates were made of the meridians of the poles. A ray-tracing study was made of the focusing of radiation escaping from possible Jovian field-aligned ducts. The effect of asymmetrical stop zones is discussed. A possible explanation of the influence of Io is offered.

## 1. Introduction

Systematic observations of the decametric radiation from Jupiter have been conducted by the University of Florida group at Gainesville since 1956, and at the Maipú Radioastronomical Observatory in Chile since 1959. Monitored recordings are regularly made with simple calibrated radiometers at several fixed frequencies between 5 and 52 Mc/s. Intensities of the circular polarization components are measured at three of the frequencies. Recordings of the dynamic spectra and detailed structure of bursts are made

during the more intense noise storms. The purpose of this paper is to present some of the more recent results of the observational program, and of related theoretical investigations.

## 2. Average Spectra

One of the objectives of the program has been the determination of the average spectral distribution of the decametric radiation occurring during an entire apparition. Such a spectrum is shown in figure 1.